IL NUOVO CIMENTO **39 C** (2016) 378
DOI 10.1393/ncc/i2016-16378-6

COLLOQUIA: IWM-EC 2016

Probing the nuclear symmetry energy at high densities with nuclear reactions

Y. LEIFELS(*)

GSI Helmholtzzentrum für Schwerionenforschung - Planckstr. 1, 64291 Darmstadt, Germany

received 10 January 2017

Summary. — The nuclear equation of state is a topic of highest current interest in nuclear structure and reactions as well as in astrophysics. The symmetry energy is the part of the equation of state which is connected to the asymmetry in the neutron/proton content. During recent years a multitude of experimental and theoretical efforts on different fields have been undertaken to constraint its density dependence at low densities but also above saturation density ($\rho_0 = 0.16\,\mathrm{fm}^{-3}$). Conventionally the symmetry energy is described by its magnitude S_v and the slope parameter L, both at saturation density. Values of $L = 44$–$66\,\mathrm{MeV}$ and $S_v = 31$–$33\,\mathrm{MeV}$ have been deduced in recent compilations of nuclear structure, heavy-ion reaction and astrophysics data. Apart from astrophysical data on mass and radii of neutron stars, heavy-ion reactions at incident energies of several 100 MeV are the only means do access the high density behaviour of the symmetry energy. In particular, meson production and collective flows upto about 1 A GeV are predicted to be sensitive to the slope of the symmetry energy as a function of density. From the measurement of elliptic flow of neutrons with respect to charged particles at GSI, a more stringent constraint for the slope of the symmetry energy at supra-saturation densities has been deduced. Future options to reach even higher densities will be discussed.

1. – Introduction

The nuclear matter equation of state (EOS) is one of the central topics in nuclear physics. It defines the structure of nuclei, the evolution of nuclear reactions and the characteristics of compact stars. A theoretical determination of the nuclear EOS from first principles by microscopic calculations is difficult and a subject of current scientific research. However, meaningful constraints to the nuclear EOS can be obtained by laboratory experiments and astrophysical observations.

(*) Work was performed together with the ASY-EOS Collaboration

The nuclear EOS describes the relation between density, pressure, energy, temperature and the isospin asymmetry $\delta = (\rho_n - \rho_p)/\rho$, where ρ_n, ρ_n, and ρ are neutron, proton and nuclear matter densities, respectively. It is conventionally divided into a symmetric matter part independent of the isospin asymmetry and an isospin term, also quoted as symmetry energy $E_{sym}(\rho)$, that enters with a factor δ^2 into the equation of state [1]. In this description, the symmetry energy is the difference in the energy between symmetric matter $\rho_n = \rho_p$ and pure neutron matter. Different density dependences of $E_{sym}(\rho)$ can be described quantitatively by expanding the symmetry energy in terms of $(\rho - \rho_0)/\rho_0$ using the value of $E_{sym,0} = E_{sym}(\rho = \rho_0)$ and the slope parameter at normal nuclear matter density $L = 3\rho_0 \frac{\delta E_{sym}(\rho)}{\delta \rho}|_{\rho=\rho_0}$ leading to the following equation:

$$E_{sym}(\rho) = E_{sym,0} + \frac{L}{3}\left(\frac{(\rho - \rho_0)}{\rho_0}\right) + \frac{K_{sym}}{18}\left(\frac{(\rho - \rho_0)}{\rho_0}\right)^2 + ..., \tag{1}$$

where K_{sym} is referred to as curvature parameter.

Microscopic calculations of the energy functional of nuclear matter employing different approaches to the nucleon-nucleon interaction predict rather different forms of the EOS. In particular, the symmetry energy shows very different behaviours. Most calculations coincide at or slightly below normal nuclear matter density, which demonstrates that constraints from finite nuclei are active for an average density smaller than saturation density and surface effects play a role. In contrast to that extrapolations to supra-normal densities diverge dramatically. The density dependence of the nuclear symmetry energy is an important constituent for drip lines, masses, densities, and collective excitations of neutron-rich nuclei [2, 3], flows and multi-fragmentation in heavy-ion collisions at intermediate energies [1, 4], but also for astrophysical phenomena like supernovae, neutrino emission, and neutron stars [5], where knowledge on the high-density dependence of the nuclear symmetry energy is most important.

In a recent compilation, many results of nuclear structure and nuclear reaction measurements as well as astrophysical observations have been collected [6]. The authors could determine the energy at saturation density $E_{sym,0}$ and the slope parameter L to be $E_{sym,0} = 31.6 \pm 2.7\,\mathrm{MeV}$ and $L = 59 \pm 16\,\mathrm{MeV}$, despite the quite large variations in the individual measurements. However, L and $E_{sym,0}$ cannot be determined individually in most experiments, which means that a larger value of L is compensated by a smaller $E_{sym,0}$ or vice versa. Measurements may yield positive or negative values for $\mathrm{d}L/\mathrm{d}E_{sym,0}$ [7] depending on the type of the observable. The authors of ref. [7] have extracted experimental constraints from nuclear physics and astrophysical measurements in the $E_{sym,0}$–L plane by employing a hydro-dynamical model and give a consensus region of $44\,\mathrm{MeV} < L(\rho_0) < 66\,\mathrm{MeV}$ and $31\,\mathrm{MeV} < E_{sym,0} < 33\,\mathrm{MeV}$ with 68% confidence, which is in mutual agreement with the results quoted in [6].

Rather precise values of the symmetry energy has been evaluated recently for ρ/ρ_0 0.6–0.7 by Brown [8] by fitting the properties of double magic nuclei and Zhang and Chen [9]. Together with the results of an analysis of isobaric analogue states [10] and from heavy ion reaction data [4], one obtains a quite consistent behavior of the density dependence of the symmetry energy at low densities, those data are compiled in [11].

The symmetry energy at higher densities $\rho > \rho_0$ can be accessed by the determination of the mass and the radii of neutron stars [7] or by employing observables in heavy-ion collisions which are related to the early, high density phase of the reactions and its isospin content. Microscopic transport calculations predict that for a short time period

20 fm/c densities up 3 ρ_0 are reached in the central zone of a heavy-ion collision even at moderate energies $\approx$ 1 A GeV [1]. At lower energies around 200 A GeV upto $2\rho/\rho_0$ may still be reached. However, one should be aware that the highest density reached during a heavy-ion collision is not necessarily equivalent to the density which is probed by a certain observable. This question has to be addressed when extracting constraints on the density dependence of the symmetry energy from experimental data.

A multitude of observables have been proposed to be sensitive to the symmetry energy (for a review see [1]): ratio of multiplicities or spectra of isospin partners (*e.g.*, π^-/π^+, n/p or t/^{3}He) and the comparison of their flows: The ratio of positively and negatively charged pions measured close to or below the production threshold in the NN system ($E_{beam,thr} = 280$ MeV) is one of the observables discussed. It is predicted to be sensitive to the density dependence of the symmetry energy. Indeed, model predictions obtained with the transport code IBUU4 [12] could only reproduce existing experimental data on pion production around $E_{beam} = 400$ A MeV in various collisions systems [13] when a rather soft density dependence of the symmetry energy was applied. This can be easily understood: to account for measured dependence of the π^-/π^+ ratio with respect to collision energy and N/Z of the colliding system, a small symmetry energy at the relevant densities is needed which leads to more neutrons in the dense zone and —consequently— a larger number of nn-collisions enhancing the number of π^- to the measured value. Incorporation of in-medium effects like mass-shifts of the pions, pion potentials, s-wave production of pions, and the properties of intermediate Delta resonances may lead to different and even opposite conclusions [14, 15], while describing the experimental data equally well. Obviously pion production is sensitive to the symmetry energy but at the moment it is not completely settled how this influences the experimental data. A way-out would be to study not pion ratios but double ratios of pion production, *i.e.* comparing pion ratios in a neutron rich and proton rich system having the same Z. Here, some input parameters to the models will drop out. Such experiments have been accomplished at the Riken facility with the BIGRIPS magnet and the SPIRIT TPC, recently.

Other observables which are sensitive to the symmetry energy at supra-normal densities are collective flows. At energies below 1 A GeV the reaction dynamics is largely determined by the nuclear mean field. The resulting pressure produces a collective motion of the compressed material whose strength will be influenced by the symmetry energy in isospin-asymmetric systems.

2. – Neutron and charged particle elliptic flow

The strengths of collective flows in heavy ion collisions are determined by a Fourier expansion of the azimuthal distributions of particles around the reaction plane:

$$\frac{\mathrm{d}\sigma(y)}{\mathrm{d}\phi} = C(1 + 2v_1(y)\cos\phi + 2v_2(y)\cos 2\phi.....). \tag{2}$$

The side flow of particles is characterized by the coefficient v_1 and the elliptic flow by v_2. The value of v_2 around mid-rapidity is negative at incident beam energies between 0.2 and 6 A GeV which signifies that matter is squeezed out perpendicular to the reaction plane. Elliptic flow at those energies is known to be sensitive to the stiffness of the symmetric part of the nuclear equation of state. In fig. 1 data for the elliptic flow v_2 of protons emitted around mid-rapidity in Au+Au collisions [16] are shown as a function of beam energy together with predictions of the IQMD model employing a hard (HM) and

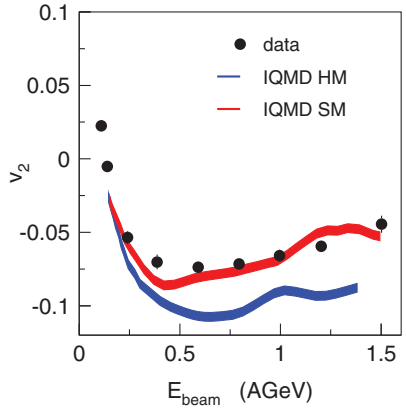

Fig. 1. – (Color online) Elliptic flow v_2 of protons as a function of beam energy for Au+Au collisions and semicentral collisions [16]. The data points are shown as full circles, predictions by the IQMD model for a soft and a hard nuclear equation of state with momentum-dependent interactions by red and blue bands, respectively. The data are selected for particles around mid-rapidity ($|Y^0| < 0.2$) and high transverse momenta ($u_t^0 > 0.8$), where u_t is the transverse component of the four velocity u, $u_t = \beta_t\gamma$. The 3-vector β is the velocity in units of the light velocity and $\gamma = 1/\sqrt{1-\beta^2}$. Scaled units are used $Y^0 = y/y_p$ and $u_t^0 = u_t/u_p$, with $u_p = \beta_p\gamma_p$, the index p referring to the incident projectile in the center-of-mass system. In these units the initial target-projectile rapidity gap always extends from $Y^0 = -1$ to $Y^0 = 1$ [16,17].

a soft (SM) nuclear equation of state augmented by a momentum-dependent interaction, which has been fitted to experimental scattering data [17]. The data are best described by a soft (SM) equation of state. The larger negative v_2-values for a hard equation of state are almost completely due to the higher density gradients perpendicular to the reaction plane and, therefore, an effect of the acting potentials.

The ratio of elliptic flow strengths of neutrons and light charged particles has been proposed as an robust observable sensitive to the EOS of asymmetric matter [18]. Neutron and proton emission has been measured by a combination of the LAND neutron detector with a part of the FOPI set-up [19,20]. A reanalysis of the data and comparison to the results of the UrQMD transport model [21] yielded a moderately soft symmetry energy dependence on density, $L = 86 \pm 15$ MeV. Despite the large error, a particular soft or a very stiff density dependence of the symmetry energy could be ruled out. These results have been confirmed by using a different transport code [22]. Nevertheless, the statistical error bars of the data are rather large, and, therefore, an attempt was started by the ASY-EOS collaboration to remeasure the neutron/proton flow in Au+Au collisions at an incident energy $E_{beam} = 400$ A MeV.

2˙1. *The ASY-EOS experiment.* – The set-up of the ASY-EOS experiment at the SIS18 accelerator is presented in fig. 2. Upstream from the target, a thin plastic scintillator foil was placed for measuring the beam particles and serving as a start detector for the time-of-flight systems. The granular and high-efficient neutron detector LAND [23] was placed close to 45° with respect to the beam direction. A veto wall of thin plastic scintillator material in front of LAND was used to discriminate between neutrons and charged particles. The Krakow Tripple Telescope Array (KRATTA [24]) was placed opposite to LAND covering approximately the same angular acceptance. This device allows to identify light charged fragments.

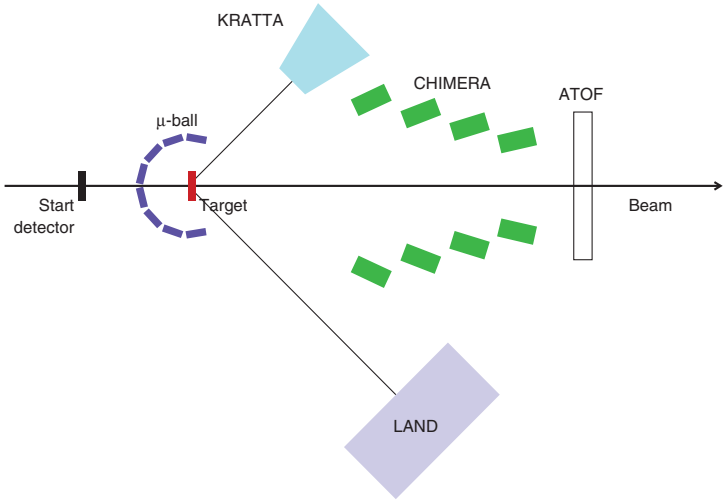

Fig. 2. – (Color online) Sketch of the setup of the ASY-EOS experiment (S394) at the SIS18 of GSI showing the six main detector systems and their positions relative to the beam direction. Dimensions and distances are not to scale (from ref. [26]).

Three detector systems were used for event characterization and back ground suppression. The ALADIN Time-of-Flight (ATOF) detected charged particles and fragments emitted at very small polar angles $\Theta_{lab} < 7^\circ$ close to beam. Four double rings of the CHIMERA multidetector [25] consisting out of 352 CsI(Tl) scintillators were placed in forward direction, and the target was surrounded by four rings with 50 thin CsI(Tl) elements of the Washington University Microball array. Those detectors provided sufficient granularity and solid angle coverage to determine the orientation of the reaction plane and the impact parameter. A detailed description of the setup is available in [26].

2˙2. *Experimental results.* – The data analysis procedure is described in detail in [26]. The v_2 ratios obtained for neutrons v_2^n and light charged particles v_2^{ch} after applying all corrections are shown in fig. 3. Constraints to the symmetry energy were obtained by comparing the ratio v_2^n/v_2^{ch} with corresponding UrQMD predictions.

A soft iso-scalar EOS was chosen for the calculations and the following parameterization was used for the density dependence of the symmetry energy:

$$E_{sym}(\rho) = E_{sym}^{pot}(\rho) + E_{sym}^{kin}(\rho) = 22 \text{ MeV}(\rho/\rho_0)^\gamma + 12(\rho/\rho_0)^{2/3} \text{ MeV} \tag{3}$$

with $\gamma = 0.5$ and $\gamma = 1.5$ corresponding to a soft and a stiff density dependence, respectively.

The two predictions obtained under these conditions are presented in fig. 3 together with the experimental results. The parameters which describe the data best are obtained by fitting a linear interpolation between the two predictions. The resulting power-law coefficient is $\gamma = 0.75 \pm 0.10$. The corresponding v_2 ratio is shown as black line in fig. 3. In comparison with the FOPI-LAND data, the statistical accuracy of the ASY-EOS experiments represents an improvement by a factor of 2. A systematic uncertainty arose from occasional malfunction of the electronic circuits for the time measurement with LAND. It prohibits extending the data evaluation into the region of large transverse momenta. For

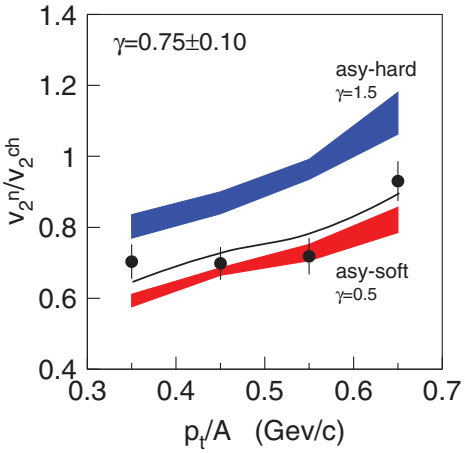

Fig. 3. – (Color online) Elliptic flow ratio of neutrons over charged particles measured in the same acceptance range for central ($b < 7.5$ fm) Au+Au collisions at 400 A MeV as a function of transverse momentum, p_t/A. The black circles represent the experimental data. The blue and red bands represent the results of UrQMD model calculations employing a hard and soft density dependence of the symmetry energy. Fitting a linear interpolation between the two extremes to the experimental data yields a γ-value $\gamma = 0.75 \pm 0.10$. The black line shows the resulting predictions.

this reason this analysis is restricted to $p_t < 0.7$ GeV/c. Another uncertainty is related to the lower energy threshold for neutron detection. The necessary corrections and the methods used for estimating the remaining errors are described in detail in ref. [26].

With all corrections and errors included, the acceptance-integrated elliptic flow values lead to a power-law coefficient $\gamma = 0.72 \pm 0.19$. The corresponding slope value is $L = 72 \pm 13$ MeV. Changing the absolute value of the symmetry energy at ground state nuclear matter density in the simulations to a lower value, $E_{sym}(\rho_0) = 31$ MeV, results in a lower γ-value $\gamma = 0.68 \pm 0.19$. This is still within the error bar of the above result.

This result is displayed in fig. 4 (right panel) where the symmetry energy is shown as a function of reduced density ρ/ρ_0 together with various microscopic model predictions [27]. The experimental data are represented as coloured bands. The results of the FOPI-LAND experiment are shown in yellow and the one of the ASY-Experiment in orange. Microscopic many-body calculations, DBHF, and variational calculations, var AV_{18}, are compared to phenomenological approaches (NL3, DD-TW and DD-$\rho\sigma$) and two Skyrme interactions (SKM* and SKL ya). The figure illustrates how well the findings of this analysis can discriminate between the models. A moderately soft density dependence of the symmetry energy is predicted by various microscopic calculations, *e.g.*, variational calculations employing an Argonne potential including three-body forces or relativistic mean field calculations (DD-TW). For completeness the calculations from ref. [27] for the EOS of symmetric matter are shown in the left panel of fig. 4 together with the experimental constraint from the FOPI collaboration [28] employing elliptic flow of protons and light charged particles in Au+Au collisions between 0.25 and 1.5 A GeV.

2˙3. *Density tested in the ASY-EOS experiment.* – Since microscopic transport models are reproducing reasonably well the experimental data it seems to be appropriate to

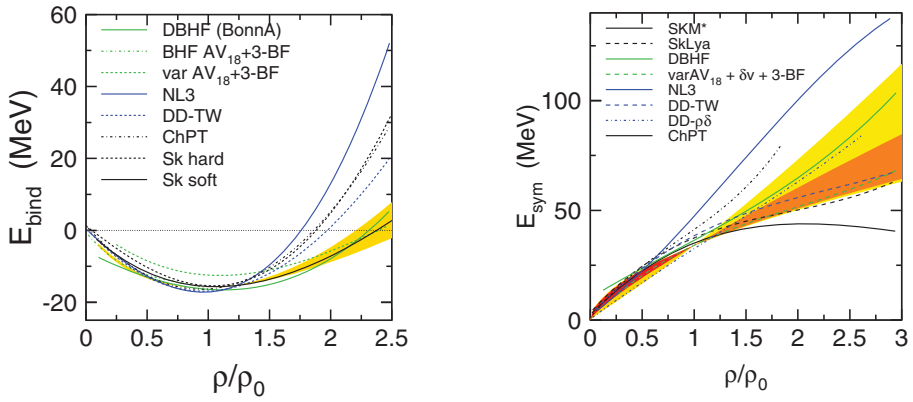

Fig. 4. – (Color online) Left panel: Constraints from experimental data of the FOPI collaboration as presented in [28] (yellow area) are shown together with predictions of microscopic model calculations employing different methods and different interactions [27]. Right panel: Result of the ASY-EOS experiment (orange area) and the FOPI-LAND analysis (yellow area) together with theoretical predictions for $E_{sym}(\rho)$ using different approaches: Dirac-Brückner-Hartree-Fock calculations (DBHF), Relativistic Mean Field (DD-TW and DD-$\rho\delta$), and two Skyrme predictions (SKM* and SkLya). The calculations are taken from [27].

deduce the density range relevant for the sensitivity to the symmetry energy in this reaction by using one of those codes. For this investigation the Tübingen Version of the QMD model, TüQMD, [22] was chosen (see [26] for more details). In this study the following prescription was used: Two calculations were performed with a moderately soft and a hard symmetry energy dependence in a given density range and the same, an intermediate, linear dependence on density, every where else. The magnitude of the difference in the elliptic flow ratio of neutrons and charged particles for those two calculations was taken as a measure of the relevance of the specific density region for the determination of the symmetry energy. The two density dependences of the symmetry energy, hard and soft (blue and red lines in fig. 5, respectively), are shown in the left panel of fig. 5 together with the linear form (black line) used as default parameterization.

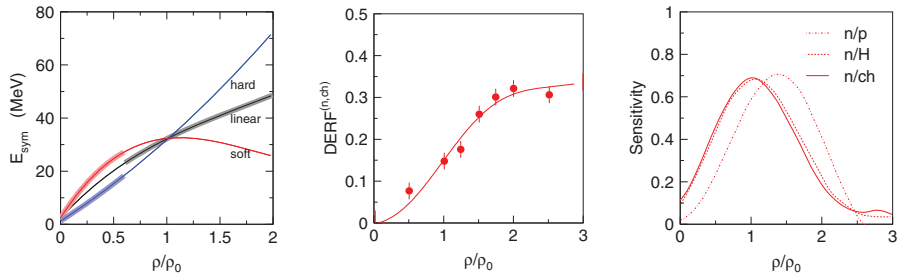

Fig. 5. – (Color online) Left panel: The different parametrizations describing the density dependence of the symmetry energy which were used for the investigation described in the text. The linear one was employed as a normal or default form of $E_{sym}(\rho)$. Middle panel: The function $DERF(\rho)$ for the ratio of elliptic flows of neutrons and charged particles. Right panel: Derivative of $DERF(\rho)$ as a function of density. These results are taken from [26].

To quantify the results, the function $DERF$ (Difference of elliptic flow ratio) is defined:

$$DERF^{n,Z}(\rho) = \frac{v_2^n}{v_2^Z}(hard, \rho) - \frac{v_2^n}{v_2^Z}(soft, \rho). \tag{4}$$

An example of the function $DERF(\rho)$ is presented in the middle panel of fig. 5. At zero density $DERF(0)$ is zero by definition and at high densities $DERF(\rho)$ is approaching the maximal value, which is the variation of v_2 for the two options of the symmetry energy. The region in density where $DERF(\rho)$ is changing most rapidly is also the density regime which is most relevant for the determination of the symmetry energy. Hence, the value of the derivative $\mathrm{d}DERF(\rho)/\mathrm{d}\rho$ is a measure of the impact of the symmetry energy on the elliptic flow observables. In the right panel of fig. 5 the derivative of $DERF(\rho)$ is shown for three choices of the elliptic flow ratio, namely for protons (n/p), hydrogen isotopes (n/H) and all charged particles (n/ch).

It can be seen in the figure that the maximum sensitivity achieved with the elliptic flow ratio of neutrons to charged particles is reached close to saturation density and extends beyond twice this value. This finding is in agreement with results of [28] which were obtained by analyzing also elliptic flow data of charged particles and employing the Quantum Molecular Model code IQMD [17]. For ^{197}Au + Au collisions at 400 A MeV the force-weighted density, defined by the authors, is spread over a broad density regime extending from $0.8 < \rho/\rho_0 < 1.6$.

The derivative of $DERF(\rho)$ for the neutron-proton ratio peaks at a higher value, 1.4 to $1.5\rho_0$. This observation gives rise to the expectation that with sufficient isotope separation one would be able not only to constraint the slope of the symmetry energy but also its curvature. Theoretical models should permit to adjust slope and curvature parameters of the symmetry energy independently. In addition, it should be possible to access the symmetry energy also at higher densities by rising the beam energy.

3. – Conclusions and outlook

The symmetry energy at supra-saturation densities can be effectively probed with the elliptic flow ratio of neutrons and charged particles. The ASY-EOS collaboration measured data for Au+Au collisions at 400 A MeV, and a slope for the of $L = 72 \pm 13$ for the density dependence of the symmetry energy could be deduced from the v_2 ratio of neutrons and charged particles. According to model predictions, similar observables might also be sensitive not only to the slope of the symmetry energy but also to its curvature at high densities. Hence, it would be interesting to measure n and light charged particle flow also at higher energies and for different systems. In collisions of Sn-isotopes one could investigate the evolution of the v_2 ratio as a function of N/Z of the colliding system.

How the sensitivity of the various observables to the symmetry energy develops with rising beam energy and larger densities is by no means obvious and more calculations using different models and prescriptions need to be performed. Particle production is predicted to be most sensitive to modifications in the neutron/proton density close to threshold. The η meson has a production threshold of $E_{thr,NN} = 1.22\,\mathrm{GeV}$ in the NN system and it was shown that the η production is sensitive to the density dependence of the symmetry energy upto approximately 5 A GeV incident energy [29]. Kaon production below and close to threshold ($E_{thr,NN} = 1.6\,\mathrm{GeV}$ has proven to be sensitive to the density reached in the course of the collision. It has been shown in particular that

kaon yields are robust observables to constrain the iso-scalar EOS. At sub-threshold energies kaons are produced in the central high-density region and, because they are not re-absorbed by the surrounding nuclear matter, they are true messengers of the dense overlap zone. The production ratio (K^+/K^0) is predicted to be sensitive to the symmetry energy and, therefore, may be an interesting observable accessing densities beyond twice the saturation density. An experiment studying Au+Au reactions at 1.25 A GeV was performed by the HADES collaboration. The HADES detector set-up allows not only for measuring charged kaons but also reconstructing K^0 by their decay into charged pions with high accuracy. Sufficient statistic was accumulated and the data analysis is currently being finalized.

Symmetry effects are very small, because the contribution of the symmetry energy enters with a factor δ^2 into the equation of the state of nuclear matter. Since δ is rather small even for the most neutron rich stable isotopes it is evident that those studies have to be extended to radioactive beams with enhanced neutron-proton asymmetry. Experimental facilities, *e.g.* RIKEN/RIBF, MSU/FRIB, GANIL/SPIRAL2 are or will become available, which allow further studies of the symmetry energy by different experimental methods. But the highest energies and consequently highest densities will be accessed with FAIR/SFRS facility. The super fragment separator will have a magnetic rigidity of 20 Tm and will provide radioactive beams upto 1 A GeV. This will offer the possibility to study the symmetry energy at high densities.

* * *

Results presented in this contribution have been obtained within the ASY-EOS Collaboration. See ref. [26] for a complete list of authors.

REFERENCES

[1] Li Bao-An, Chen Lie-Wen and Ko Che Ming, *Phys. Rep.*, **464** (2008) 113.
[2] Brown B. A., *Phys. Rev. Lett.*, **85** (2000) 5296.
[3] Roca-Maza X., Centelles M., Viñas X. and Warda M., *Phys. Rev. Lett.*, **106** (2011) 252501.
[4] Tsang B. *et al.*, *Phys. Rev. Lett.*, **102** (2009) 122701.
[5] Steiner A. W. *et al.*, *Phys. Rep.*, **411** (2005) 325.
[6] Li Bao-An and Han X., *Phys. Lett. B*, **727** (2013) 276.
[7] Lattimer J. M. and Steiner A., *Eur. Phys. J. A*, **50** (2014) 40.
[8] Brown B. A., *Phys. Rev. Lett.*, **111** (2013) 232502.
[9] Zhang Z. and Chen L. W., *Phys. Lett. B*, **726** (2013) 234.
[10] Danielewicz P. and Lee J., *Nucl. Phys. A*, **922** (2014) 1.
[11] Horrowitz C. J. *et al.*, *J. Phys. G: Nucl. Part. Phys.*, **922** (2014) 1.
[12] Xiao Z. *et al.*, *Phys. Rev. Lett.*, **102** (2009) 062502.
[13] Reisdorf W. *et al.*, *Nucl. Phys. A*, **781** (2007) 459.
[14] Feng Z. Q. and Jin G. M., *Phys. Lett. B*, **683** (2010) 140.
[15] Hong J. and Danielewicz P., *Phys. Rev. C*, **90** (2014) 024605.
[16] Reisdorf W. *et al.*, *Nucl. Phys. A*, **876** (2012) 1.
[17] Hartnack C. *et al.*, *Eur. Phys. J. A*, **1** (1997) 151.
[18] Russotto P. *et al.*, *Phys. Lett. B*, **697** (2011) 471.
[19] Leifels Y. *et al.*, *Phys. Rev. Lett.*, **71** (1993) 963.
[20] Lambrecht D. *et al.*, *Z. Phys. A*, **350** (1994) 115.
[21] Li Q. *et al.*, *J. Phys. G*, **32** (2006) 407.
[22] Cozma M. D., *Phys. Lett. B*, **700** (2011) 139.
[23] Blaich T. *et al.*, *Nucl. Instrum. Methods Phys. Res. A*, **314** (1992) 136.

[24] Lukasik J. *et al.*, *Nucl. Instrum. Methods Phys. Res. A*, **709** (2013) 120.
[25] Pagano A. *et al.*, *Nucl. Phys. A*, **734** (2004) 504.
[26] Russotto P. *et al.*, *Phys. Rev. C*, **94** (2016) 00022.
[27] Fuchs C. and Wolter H., *Eur. Phys. J. A*, **30** (2006) 5.
[28] Le Fèvre A. *et al.*, *Nucl. Phys. A*, **945** (2016) 112.
[29] Yong G. and Li Bao-An, *Phys. Lett. B*, **723** (2013) 388.